Effect of annealing temperature on the structural and optical properties of ZnS thin films deposited by CBD

Mohammad M. Ali*

Department of Physics, College of Science, University of Basra, Iraq

mohammadali434@yahoo.com

Abstract

Zinc sulfide thin films were deposited on glass substrates by using chemical bath deposition (CBD) technique at 90^{o}Cand annealed at different temperatures (250, 300 and 350^{o}C) in air for 30 minutes. The chemical bath contains the solutions of thiourea, zinc sulphate, ammonia and hydrazine hydrate. Effect of annealing temperature on the microstructure and optical properties of ZnS thin films were investigated. The structural and optical properties of ZnS thin films were characterized using X-ray diffraction [XRD] and UV-Visible-NIR spectrometry. The XRD analyses indicate that ZnS thin films have zinc blende (cubic) structures with (111) preferential orientation. The structural parameters like lattice parameter, crystallite size, micro strain and dislocation density are calculated. The crystallinity is apparently improved with the increase of annealing temperature. The average grain size was found to be 1.9198 nm and after annealing the grain size was 2.1612 nm, 4.2821 nm and 5.7720 nm respectively (grain size increase with the increase of annealing temperatures, whereas dislocation density and micro strain decreases with the increase of annealing temperatures). It is also found that film surface changes to ZnO after the film is annealed at 300-350^{o}C. The transmittance, absorbance and reflectance are recorded in the range of 300-1000 nm, the optical band gap is direct with a value of 3.85eV, but

this value decreased to 3.42eV with annealing temperature at 350^{o}C. The result showed that the CBD ZnS thin films annealed at 350^{o}C exhibit the highest transmittance of about 95.50%. The refractive index(n), extinction coefficient(k), optical conductivity and real and imaginary parts of dielectric constant are evaluated. Additionally, the increase of annealing temperature will increase the pores in films, which results in the decrease of refractive indices and increase of extinction coefficients of the film.

Keywords: ZnS, thin films, annealing effect, structural and optical properties, band gap.

1- Introduction

2-

Recent researches on solar cells fabrication aimed towards lowering the fabrication cost in order to decrease the price of the energy obtained. The researches were directed to use thin films technology for solar cell fabrication (Nair et al. 1998). Suitable materials should be easily prepared and inexpensive, show stable behavior over long periods of operation. The high cost and the difficulty to obtain single crystal semiconductors give a great interest to polycrystalline semiconductors, including a wider range of compounds which could be used in different applications (Pandy et al. 1996). Generally, Cu(In,Ga)Se_2 [CIGS] solar cells are fabricated using a cadmium sulfide [CdS] buffer layer in order to protect the junction region from sputtering damage during subsequent n-type zinc oxide deposition and to modify the surface of p-type CIGS absorber (Liu et al. 2008). CdS is the most promising buffer layer for thin film hetero-junction solar cells, and the highest conversion

efficiencies have been achieved with the chemical bath-deposited CdS buffer layer in CIGS solar cells.

However, due to the toxic hazards of the production of CdS layers, many research groups have been developed Cd-free buffer layers for CIGS thin film solar cells. One of the most candidates is ZnS, which has been primarily investigated as a buffer layer in CIGS solar cell devices. ZnS film has unique physical properties, such as high refractive index, low optical absorption in the visible and infrared light range, and it has a wider band gap than CdS (Eg_{ZnS}~3.7eV and Eg_{CdS}~2.4eV), such film is widely used in many optical and electronic area. In the area of optics, ZnS can be used as reflectors and dielectric filters because of its high refractive index and high transmittance in visible range. The using of ZnS could lead to increase high-energy photons to the junction, decrease in window absorption losses and improve in the short-circuit current of the cell (Noikaew et al. 2008).Consequently, it is a potentially important material to be used as an antireflection coating for heterojunction solar cells. It is an important device material for the detection, emission and modulation of visible and near ultra violet light. It is also becomes a highly efficient luminescent material, when doped with manganese, copper or other ions (elements). Owing to wide band gap, it can be used for fabrication of optoelectronic devices such as blue light-emitting diodes, electroluminescent devices, electro optic modulator, optical coating, n-window layers for thin film heterojunction solar cell, photoconductor and especially photovoltaic devices (Ndukwe 1996, Varitimos and Tustison 1987, Yamagaet al. 1990).

The structure and properties of ZnS films are different with different deposited technique. For example, (Zhang et al. 2006) fabricated single cubic phase ZnS films by plasma-assisted metalorganic chemical vapor deposition. (Subbaiah et al. 2006) investigated the structural, electrical and optical properties of ZnS films deposited at different temperatures using close-spaced evaporation for photovoltaic applications. In the previous reports, it has been confirmed that the substrate temperature and annealing will strongly affect the structure and optical properties of the sputtered Nb_2O_5 films (Lai et al. 2005). (Roy et al. 2006) had reported the effect of annealing on structure and optical properties of ZnS films fabricated by chemical bath deposition technique. The annealing temperature will also affect the structure and optical properties of ZnS film deposited by CBD. Therefore, the effects of annealing temperature on the properties ZnS films should be well understood from a fundamental as well as from an applied point view.

Several techniques such as spray pyrolysis (Chamberlin and Skarman 1966), thermal evaporation (Porada and Schabowska 1986),chemical bath deposition (CBD) (K. Nair and S. Nair 1992), molecular beam epitaxy (Yonetaet al. 1993), metal-organic vapor phase epitaxy (Aboundiet al. 1994), and chemical vapor deposition (Kashani 1996) have been used to produce ZnS thin films. Among them, chemical bath deposition is well known as a prevalent low-temperature aqueous technique for depositing large-area thin films of semiconductors, has been recognized as the simplest and most economical one. CBD is a technique in which thin films are deposited on substrates immersed

in dilute solutions containing metal ions and the chalcogenide source. A chelating agent is used to limit the hydrolysis of the metal ion and impart some stability to the bath, which would otherwise undergo rapid hydrolysis and precipitation. The technique under these conditions relies on the slow release of chalcogen ions into the solution in which the free metal ion is buffered at a low concentration. Film formation on the substrate takes place when ionic product (IP) exceeds solubility product (SP) (KamounAllouche et al. 2010).

Using CBD method, a large number of binary compound semiconductors such as CdS, CdSe, PbS, ZnS have been deposited as thin films. In CBD for the ZnS thin films there are many variables to be controlled, including Zn source, S source, complexing agent, PH controlling agent, bath temperature, and deposition time. Due to the difficulty in suitably controlling these variables, the properties of ZnS films prepared by CBD are not stable and consistent in published works. Chemical bath deposition of ZnS thin films using ammonia (NH_3) and hydrazine hydrate (N_2H_4) as complexing agents has been reported by Dona and Herrero(Dona and Herrero 1994).The importance of ternary complexes (two ligands and one metal) for the deposition of ZnS has been studied by O'Brien et al. (O'Brien et al. 2000). Vidal et al. (Vidal et al.1999) reported the influence of NH_3 concentration on the properties of chemical bath deposited ZnS films. The effects of ammonium salt on the chemical bath deposition of ZnS thin film have been studied by Oladeji and Chow (Oladeji and Chow 1999). Trisodium citrate has also been used as complexing agent in the deposition of ZnS thin film by Cheng et al. (Cheng

et al. 2003) and Johnston et al. (Johnston et al. 2002).

In this paper, we focus on the preparation ofZnS thin films by chemical bath deposition. The influence of annealing temperatures (250^{o}C, 300^{o}C and 350^{o}C) on the structural properties of the films have been investigated, and the optical properties of the films have also been analyzed.

3- Experimental

ZnS thin films are prepared by CBD method on glass substrates (25mmx50mmx1mm). The schematic diagram of the CBD set up is shown in Fig.1. The glass substrates has been cleaned by first dipping for 30 minute into hydrochloric acid and nitric acid, cleaning in acetone with ultrasonic vibration for 20 minute,immersed into methanol solution, rinsed again with double distilled water and then cleaned with hydrofluoric acid solution (HF 5%). Finally, those are rinsed with deionized water and drying with hot air. ZnSthin films were prepared by mixing 25ml of 0.25M zinc sulphate ($ZnSO_4$) as Zn^{2+} ion source, 25ml of 3M hydrazine hydrate $(NH_2)_2$ and 25ml of 3M ammonia (NH_4OH) was used as a complexing agent to the beaker. The mixture was poured into a beaker and immersed into the heated water bath with a temperature of 90^{o}C. The mixture was stirred to ensure homogeneous solution for 10 minutes. Thereafter, 50ml of 0.4M thiourea ($SC(NH_2)_2$) as S^{2-} ion source was added into the mixed solution beaker under stirring condition with zinc to sulphur (Zn:S) molar ratio 2.5:4. Subsequently, the pre-clean substrates were dipped vertically using substrate holder in the solution for 60 minute.After completion of film deposition, the samples were removed from the beaker and immediately

rinsed with de-ionized water to remove soluble impurities and dried with nitrogen gas. The thin, uniform and colorless ZnS films were obtained. Film thickness is estimated by the double weight method (i.e. by weighting sample before and after film depositions) and thickness up to (~200 nm) could be obtained after deposition. After deposition, the deposited films are annealed at 250^{o}C, 300^{o}C and 350^{o}C for 30 minute. The effect of annealing temperature on structural and optical properties has also been studied. X-ray diffraction (XRD) spectra were recorded with an Philips Xpert PRO diffractometer using CuKα radiation (λ=1.5406 Å, with 40 KV and 20 mA) for 2θ values over 20 to 80^{o}. The optical properties of the films were characterized by a UV-Visible-NIR double beam spectrophotometer with a wavelength range from 300 to 1000 nm.

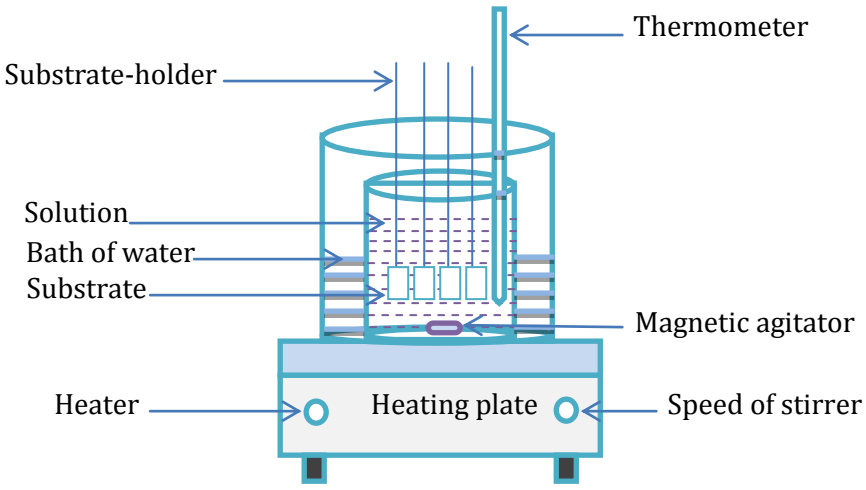

Fig.1 Chemical bath deposition (CBD) system.

3. **Result and discussion**

3.1. **Structural analysis**

Zinc sulfide exists in sphalerite, cubic and hexagonal forms. The cubic form is stable at room temperature, while the less dense hexagonal form (wurtzite) is stable above 1020^{o}C at atmospheric pressure (Gilbert et al. 2002). However, some authors have observed hexagonal structure for ZnS films obtained by CBD (Cheng et al. 2003) and the others observed cubic structure (Hasanzadeh et al. 2013, Ubale and Kulkarni 2005, Xiaochun et al. 2007, Liang-wen et al. 2013). Fig.2 shows XRD

patterns of polycrystalline ZnS thin films formed by CBD at a temperature of 90^{o}C and ZnS thin films annealed at 250^{o}C, 300^{o}C and 350^{o}C. All of the peaks for various annealing temperatures were identified to be those of the cubic ZnS phase (JCPDS card no. 79-0043) (Sahraei et al. 2008). Similar XRD pattern and structural transformation have been observed (Hwang et al. 2012, Liang-wen et al. 2013). The broad hump in the 2θ range of 20-30^{o} is due to the glass substrates.Broad peaks corresponding to improved crystallinity start to appear, as annealing temperature increases from 300^{o}C to 350^{o}C. One main peak can be observed at diffraction angle of 2θ=26.9702^{o} on the XRD spectrum obtained on the un-annealed ZnS thin film, which correspond to the cubic phase of the plane (111). Fig.2(b) shows, two main peaks at diffraction angles of 2θ=26.9707^{o} and 49.2450^{o} corresponding to the cubic planes (111) and (220) at annealed temperature 250^{o}C. A new peak appears at 2θ=31.6680^{o} as shown in Fig.2(c) with the main peak at 2θ=26.9652^{o}, also it can be shows a similar peak in Fig.2(d) at 2θ=31.6669^{o} with the

main peak at 2θ=26.4979^{o}. The new peak is due to (100) plane of ZnO according to the standard XRD-card. The main reason is that the surface of ZnS film was oxidized when it was annealed at 300^{o}C or above in air. For the as-deposited samples, the value of the lattice parameter **a** (**a**=5.4223Å) are greater than the powder sample ($\mathbf{a}_{powder}$=5.41Å), also all values of **a** for ZnS thin films annealed at 250^{o}C, 300^{o}C and 350^{o}C are greater than the powder sample (**a**=5.4774Å, 5.4860Å and 5.5262Å) respectively.

In order to obtain more structural information, the mean crystallite size (D) of the films are calculated using Scherrer formula (Warren BE 1990):

$$D = \frac{0.9\lambda}{(\beta\cos\theta)} \quad (1)$$

where λ is the X-ray wavelength (0.15406 nm), and β is the full width at half maximum [FWHM] of the film diffraction peak at 2θ, where θ is the Bragg diffraction angle. The mean crystallite size of the films were about 1.9198, 2.1612, 4.2821 and 5.7720 nm for samples deposited at 90^{o}C and annealed at 250^{o}C, 300^{o}C and 350^{o}C, respectively. These results were probably due to the crystallinity of the films being improved and the crystallite sizes becoming larger as the annealing temperatures increased.

A dislocation is a crystallographic defect, or irregularity, within a crystal structure. The presence of dislocations (δ) strongly influences many of the properties of materials. The dislocation density was calculated from the following relation (Kathirvel et al. 2009):

$$\delta = {}^{1}/_{D^{2}} \quad (2)$$

The micro strain (ε) of films were estimated using the equation (Kathirvel et al. 2009):

$$\varepsilon = \beta\cos\theta/4 \quad (3)$$

The structure parameters of ZnS thin films are summarized in Table 1. We can show from Table 1, the best temperature of annealing (Ta) is 350^{o}Cthat occurs in this temperature increase in grain size (5.7720 nm) and decreases the dislocation density and micro strain.Crystallinity is highly related to FWHM value. Valenzuela and Russer reported that the FWHM of an XRD peak is reliant on the crystallite size and lattice strain caused by the defect and/or dislocations (Valenzuela and Russer 1989). The FWHM value decreased from 4.2536^{o} to 1.4147^{o} as the annealing temperatures increased from the deposition temperature (90^{o}C) to 350^{o}C.

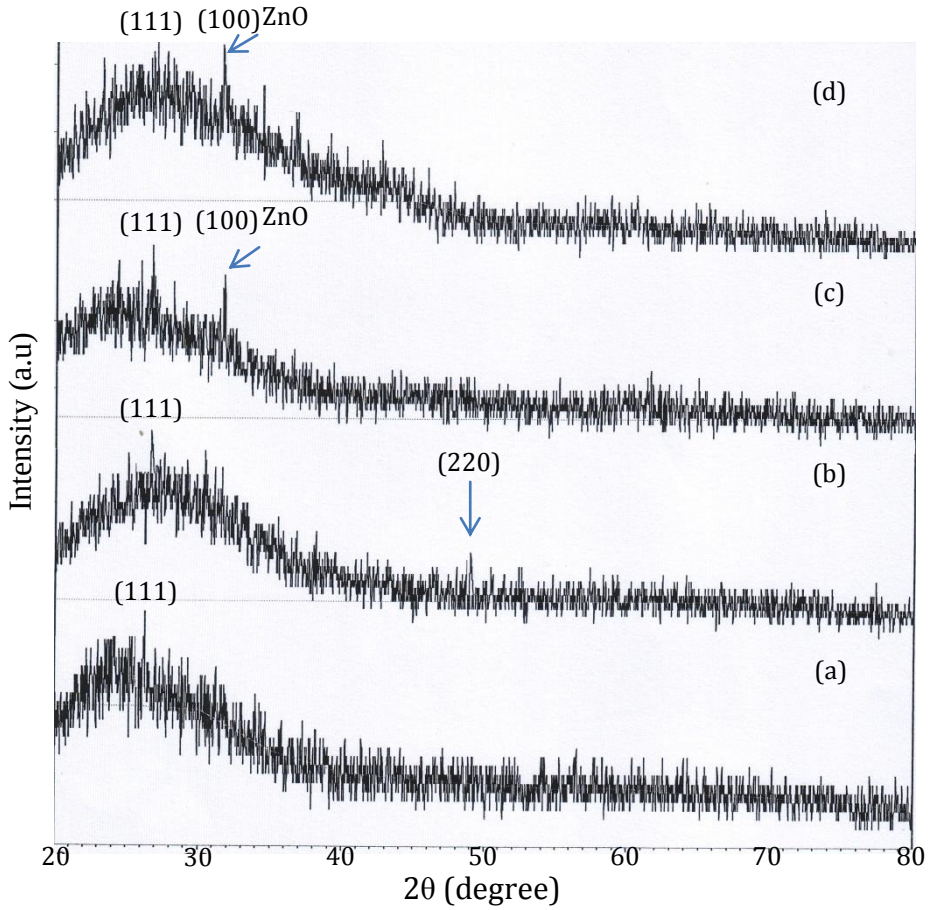

Fig. 2 X-ray diffraction patterns of ZnS thin films (a) as-deposited and annealed (b) at 250^{o}C (c) at 300^{o}C and (d) at 350^{o}C.

Table 1: Effect of annealing temperature on the structure parameters of ZnS thin films.

Sample	(hkl)	Annealing temperature (^oC)	2θ (degree)	FWHM (β)	d (Å)	Grain size D(nm)	Lattice parameter **a**(Å)	δ Lines/m^2 x10^{16}	ε x10^{-3}
ZnS(1)	(111)	unannealed	26.9702	4.2536	3.1306	1.9198	5.4223	27.1323	18.0557
ZnS(2)	(111)	250	26.9707	3.7786	3.1624	2.1612	5.4774	21.4096	16.0390
ZnS(3)	(111)	300	26.9652	1.8893	3.1673	4.2821	5.4860	5.4536	8.0949
ZnS(4)	(111)	350	26.4979	1.4147	3.1905	5.7720	5.5262	3.0015	6.0054

3.2. **Optical analysis**

The optical properties of the ZnS films deposited on glass substrates were determined from the transmission and absorption measurements in the range of 300-1000 nm. Fig. 3 shows the absorption spectra and average absorption of deposited ZnS thin films and annealed at temperatures of 250^{o}C, 300^{o}C and 350^{o}C (Note: The averages referred to in all the optical graphics in the present work was calculated in the wavelengths range from 335 to 1000 nm). It can be shows that all the samples of the ZnS films exhibit high absorbance in UV regions and low absorbance in IR regions. In the visible regions, it absorbs only slightly. This make the material to be useful as windscreen coating and driving mirror to prevent the effect of dazzling light into driver's eyes from oncoming vehicle and following vehicle. The result obtained by Nadeem and Ahmed (Nadeem and Ahmed 2000) and Ndukwe (Ndukwe 1996) on the optical absorbance of ZnS thin films for wavelength in the

infrared region showed that ZnS is practically non-absorbing in these regions which was comparedwith the result obtained in the present work.

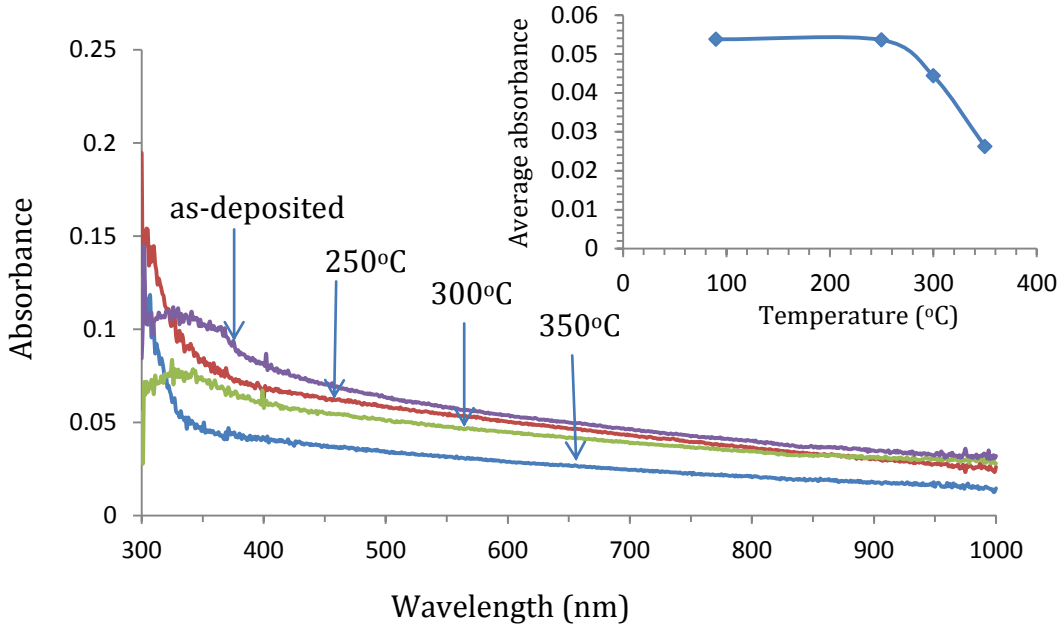

Fig. 3: Absorbance of the ZnS thin films annealed at different temperatures at the wavelength from 300 to 1000 nm with the inset is the averageabsorbance.

Fig. 4 shows the optical transmittance and average transmittance of ZnS films at different annealing temperatures. All films have high transmission, the optical properties of the ZnSthin films are very important in optimizing the growth conditions to be used as a buffer layer or window layer for solar cells. The broad cut off towards short wavelengths indicates the onset of intrinsic inter-band absorption in the ZnS. All of the cut-off wavelengths are observed at about 300 to 305 nm. The slightly blue-shift of these wavelengths directly depends on the decreasing of the deposition time and/or the film thickness and annealing temperature.

As shown in Fig. 4, the interference spectral bands shift

to shorter wavelengths (320-300) nm, and amplitude of the spectra decreases with increases annealing temperature, which is due to the variations of the structure, morphology and composition of the films after the films were annealed at high temperature. It can be seen that the transmittance (T%) increases with the increase of annealing temperature at $\lambda > 335$ nm.

The optical spectral of 350^{o}C annealed sample of ZnS films exhibit the highest transmittance of about (95.50%) in the visible spectrum. The average transmittance was about (88.49%), (89.56%), (90.08%) and (93.75%) for the ZnS films as-deposited and annealed at 250^{o}C, 300^{o}C and 350^{o}C, respectively. The film is actually an efficient transmitting and antireflective material. Because of the high optical transmission and antireflective properties of ZnS film, ZnS may play an important role in photovoltaic devices. The optical transmittances in ultraviolet-visible region of CBD ZnS films in published works are quite different, such as 80-85% (Louh and Wu 2008), more than 70% (Goudarzi et al. 2008), about 90% (Liu et al. 2008) and 80-90% (Li et al. 2010).

Fig. 5 shows the reflectance spectra of the ZnS films annealed at various temperatures on glass substrates with the average reflectance. The average reflectance was about (6.063%), (5.823%), (5.215%) and (3.099%) for the unannealedZnS films and films annealing temperatures at 250^{o}C, 300^{o}C and 350^{o}C, respectively.

The reflectance has been obtained by using the relationship (Chopra 1969, Heavens 1970):

$$R + T + A = 1 \quad (4)$$

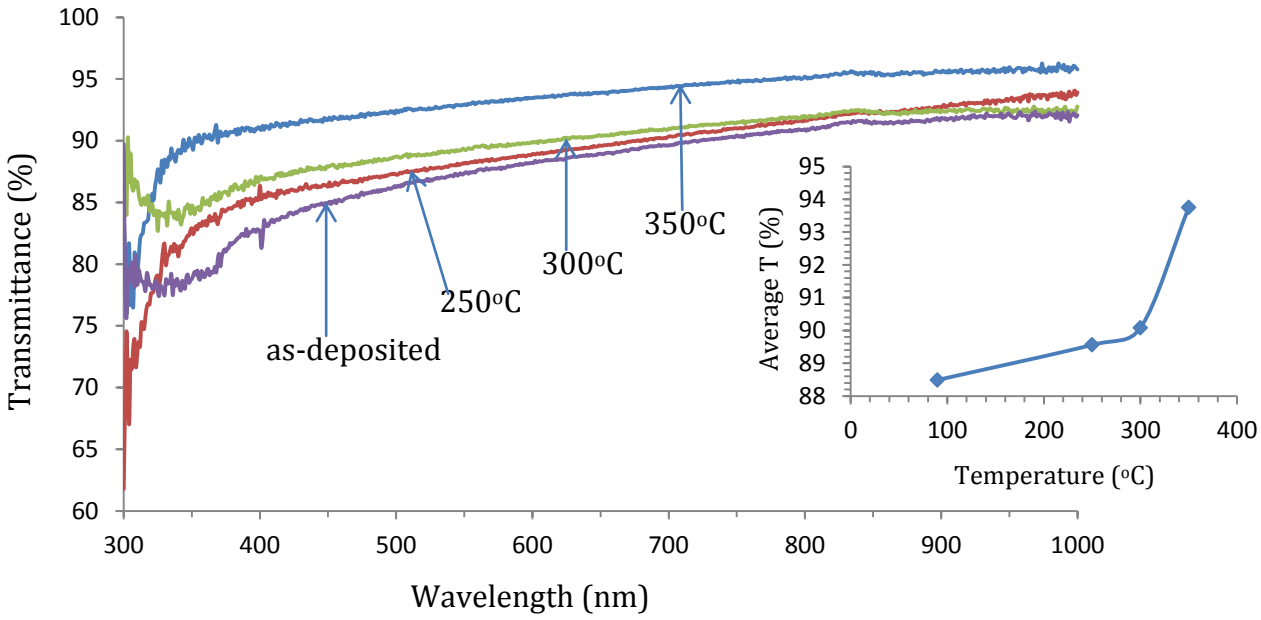

Fig. 4: Transmittances of the ZnS films annealed at different temperatures at the wavelength from 300 to 1000 nm with the inset is the average transmittance.

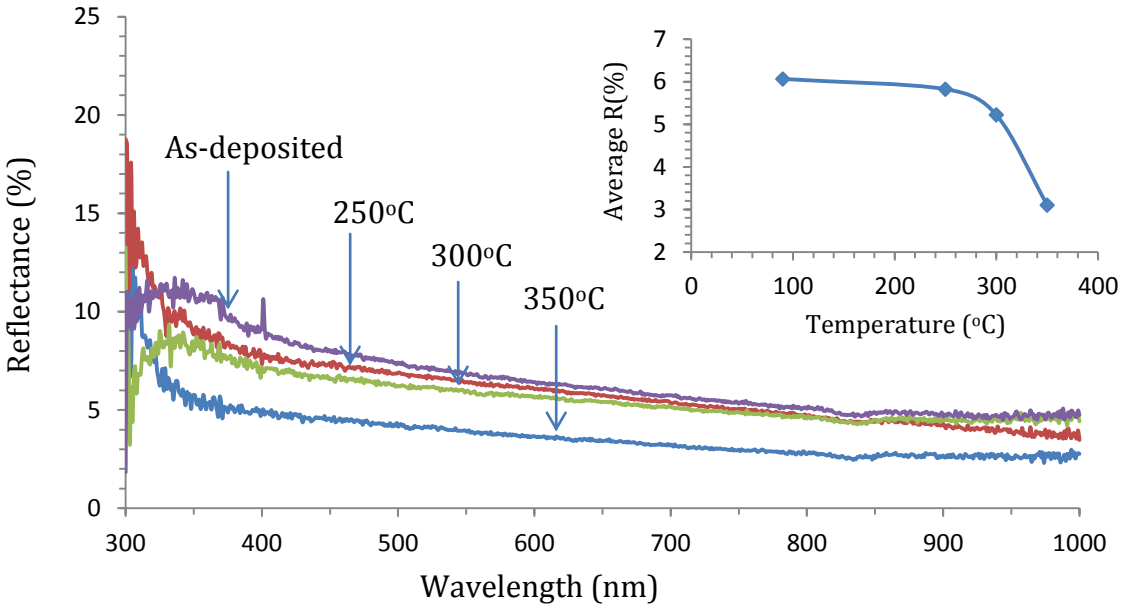

Fig. 5:Reflectance spectra as a function of wavelength of ZnS films annealed at different temperatures with the inset is the average reflectance.

The values of absorption coefficient are calculated by using the following equation (Huda Abdullah et al. 2012):

$$I_t = I_o \exp(-\alpha t) \quad (5)$$

where α is the optical absorption coefficient, t is the thickness of the film, I_t and I_o are the intensity of transmitted light and initial light respectively.

Fig. 6 shows the plot of $(\alpha h\nu)^2$ versus hν, where hν is the energy of the incident photon. The optical band gap (Eg) is calculated from the following expression by assuming a direct transition between valance and conduction bands (Tauc 1974):

$$\alpha h\nu = D(h\nu - Eg)^{1/2} \quad (6)$$

where D is a constant, and Eg is estimated by extrapolating the straight-line portion of the spectrum to a zero absorption coefficient value.

The band gap energy of the as-grown film at 90^{o}C is 3.85eV, film annealed at 250^{o}C, 300^{o}C and 350^{o}C showed the energy band gaps of 3.80eV, 3.78eV and 3.42eV, respectively. The energy band gaps ranging from 3.42eV to 3.85eV obtained in this work agree with 3.68eV by Biswass et al. (Biswass et al. 1986), 3.44eV by Lindroos et al. (Lindroos et al. 1996), 3.51-3.84eV by Nadeem et al. (Nadeem and Ahmed 2000), 3.60-3.78eV (Goudarzi et al. 2008), 3.51eV (Liu et al. 2008), 3.73-3.57eV obtained by Yildrim et al. (Yildrim et al. 2009), 3.65-3.74eV (Li et al. 2010), 3.78-3.91eV (Kang et al. 2010), 3.50-3.89eV (Shin et al. 2011) and 3.48-3.74eV by Ibiyemi et al. (Ibiyemi et al. 2012).

It could be observed that for each annealing temperature, the optical band gap was decreasing with increasing annealing temperature as shown in Fig. 7. The decrease in band gap of the films after annealing could be

attributed to improvement in the crystal structureand change grain sizes of the films after annealing temperature.

The optical properties of the prepared thin film depend strongly on the manufacturing technique. Two of the most important optical properties; refractive index and the extinction coefficient are generally called optical constants. Refractive indices and extinction coefficients of the films were determined from all normal incidence transmittance data (Lin et al. 2005). Refractive indices and extinction coefficients as a function of wavelength of the films annealed at temperatures between 250 and 350^{o}C are shown in Fig. 8 and 9, respectively. Table 3 lists the optical constants at 550 nm wavelength of the films annealed at different temperature. As can be seen in Fig. 8 and Table 3, refractive indices of the films decrease slowly as the annealing temperature increases from 250 to 350^{o}C. Accordingly, extinction coefficients increase slowly with increasing annealing temperature. Refractive indices decrease and extinction coefficient increase as the increase of the annealing temperature are due to the increase of pores and surface roughness [the movement of the atoms or molecules on film surface as the films annealed at high temperature] when films were annealed at high temperature. However, there is a sharp decrease in refractive index when the annealing temperature increases to 350^{o}C as indicated in Fig. 8. This sharp decrease in refractive index is attributed to the surface of ZnS film begins to be oxidized when film is annealed at 300-350^{o}C in air. Generally, refractive index of ZnS film (Ryu et al. 2000) and ZnO film (Mehan et al. 2004) is about 2.3 and 2.0 at 550 nm wavelength respectively.

Therefore, the surface of the film annealed at 300-350°C is ZnO, as can be seen in XRD result, which decreases the refractive index when film is annealed at 300-350°C.

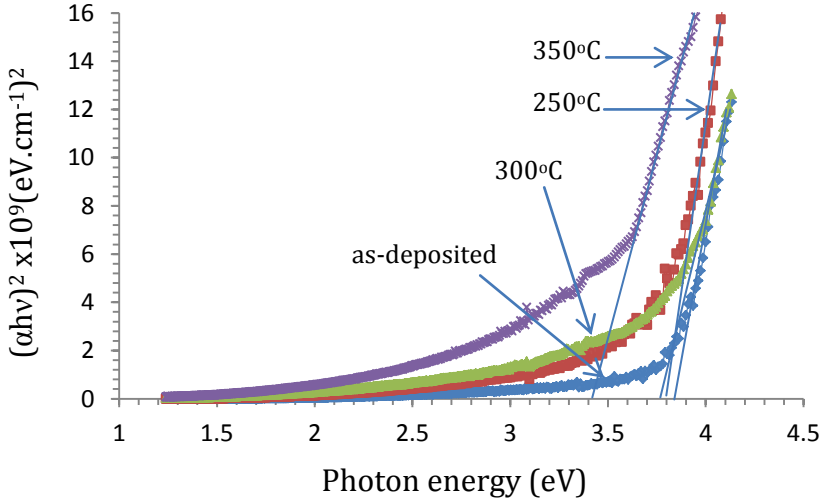

Fig. 6: The plots of $(\alpha h\nu)^2$ versus photon energy ($h\nu$) for as-deposited and annealed ZnS thin films.

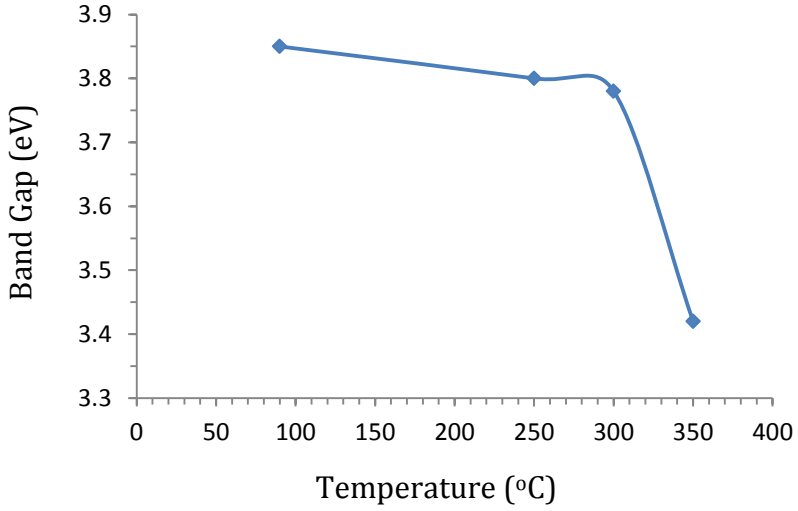

Fig. 7: Band Gap Energy of ZnS Thin Film as a Function Temperature.

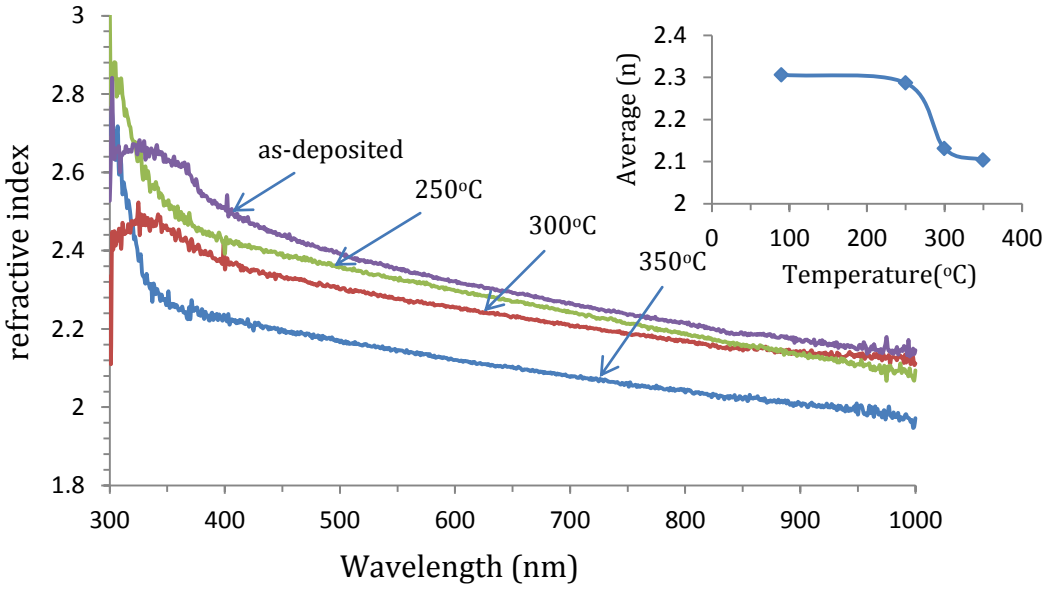

Fig. 8: Refractive indices as a function of wavelength of ZnS films at different temperatures with the inset is the average refractive indices.

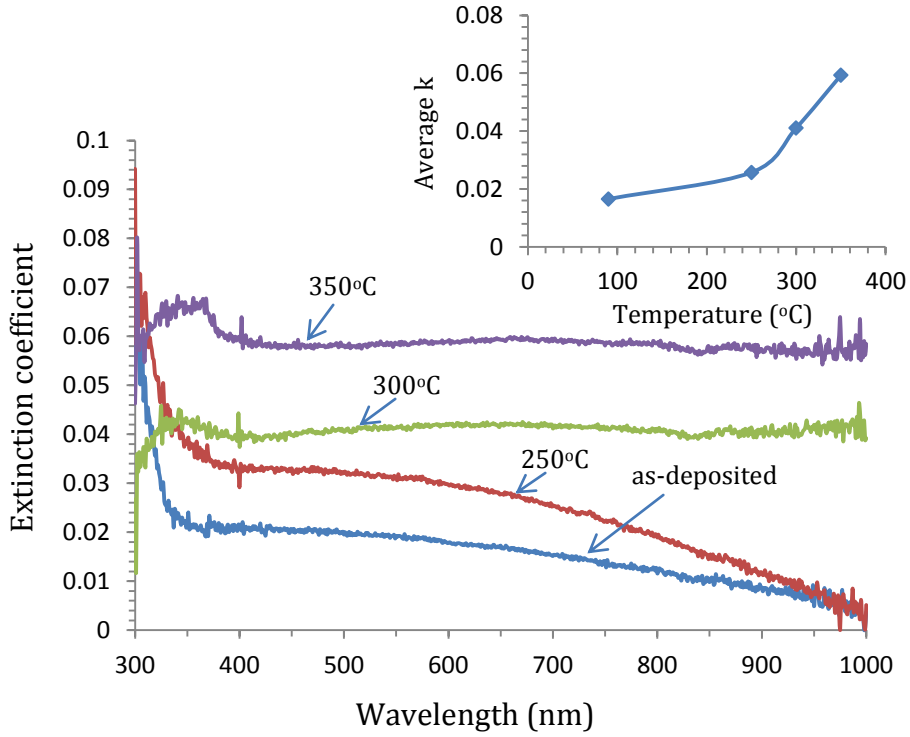

Fig. 9: Extinction coefficients as a function of wavelength of ZnS films annealed at different temperatures with the inset is the average extinction coefficient.

Table 3: Optical constants at 550 nm wavelength of ZnS films deposited at 90°C and annealed at different temperatures.

Temperature (°C)	n	k (x10^{-3})
as-deposited	2.353	19.244
250	2.328	31.235
300	2.277	41.310
350	2.146	58.439

Fig. 10 shows the variation of optical conductivity with the incident photon energy. The optical conductivity was determined using the relation (Pankove 1975):

$$\sigma = \frac{\alpha n c}{4\pi} \qquad (7)$$

where c is the velocity of light.

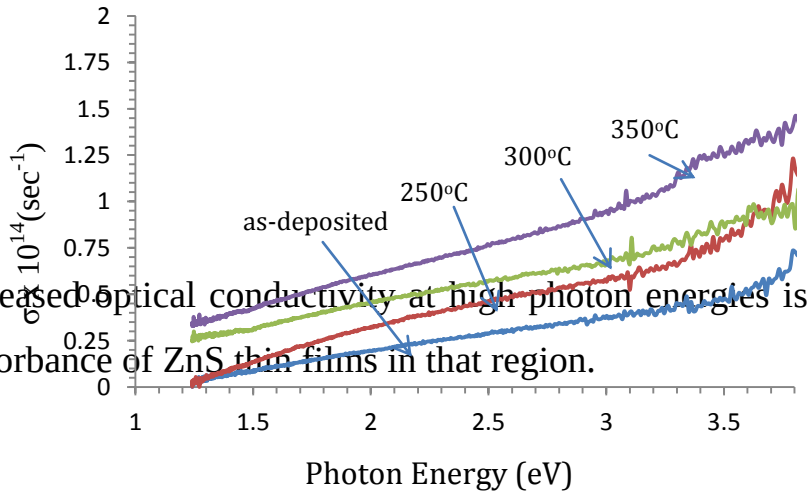

The increased optical conductivity at high photon energies is due to the high absorbance of ZnS thin films in that region.

Fig. 10: Optical Conductivity versus incident photon energy.

The real and imaginary parts of the dielectric constant were determined using the relation (Chopra 1969):

$$\varepsilon_c = \varepsilon_r + \varepsilon_i = (n + ik)^2 \quad (8)$$

where ε_r is the real part and is the normal dielectric constant (n^2-k^2), ε_i is the imaginary part and represents the absorption associated of radiation by free carrier (2nk).

Figures 11 and 12 show the variations of real and imaginary parts of the dielectric constant with the incident photon energy.

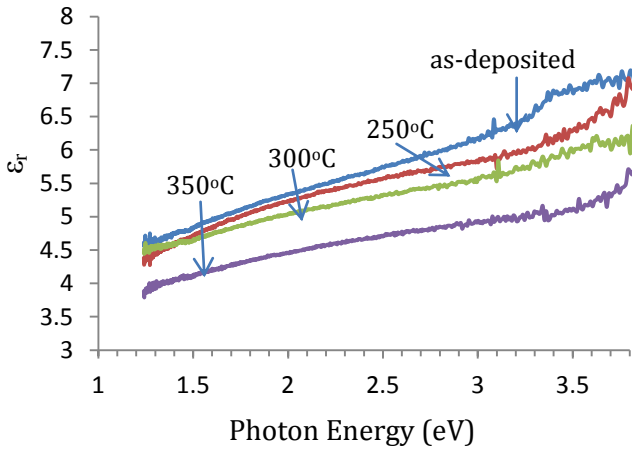

Fig. 11: Real part of the dielectric constant versus incident photon energy.

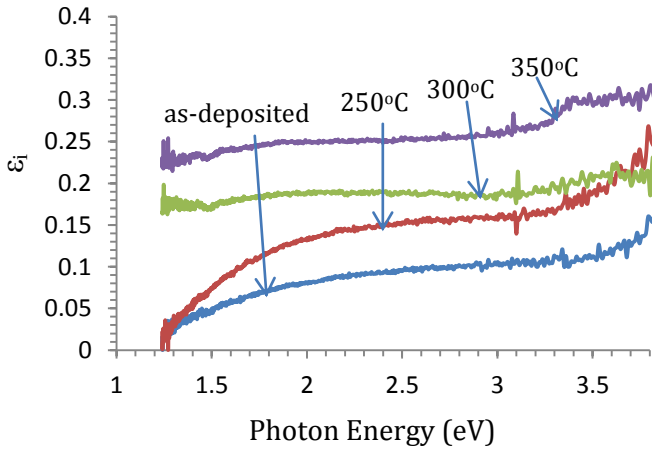

Fig. 12: Imaginary part of the dielectric constant versus incident photon energy.

4. Conclusion

Zinc sulfide thin films were prepared on glass substrates by the CBD technique. The structural and optical properties of the films deposited and annealing at different temperatures (250°C, 300°C and 350°C) were investigated. The films are in good quality, adherent and uniform. There is a good agreement between XRD and optical results. From the

experimental results, it is found that the crystallinity is apparently improved as the increase of the annealing temperatures, and we conclude that annealing of ZnS thin films reduces lattice strain, producing a more perfect crystallite and decreasing the number of micro voids. The films grown at these temperatures exhibited cubic structure. The average grains size increase from 1.9198 nm to 5.7720 nm and the optical band gap decreases from 3.85eV to 3.42eV with increasing annealing temperatures. The average transmittance increase from 88.49% to 93.75%, while reflectance decreases from 6.063% to 3.099% and increase of extinction coefficient of the film with increasing annealing temperatures. Refractive index has a sharp decrease after the film was annealed at 350^{o}C, which is due to the film surface begins to be oxidized at this temperature.

References

A. Aboundi, M. Diblasio and D. Bouchara, (1994) Phys. Rev., **B50**, 11677.

A. A. Ibiyemi, M. Tech and A. O. (2012) Awodugba, The Pacific Journal of Science and Technology, **13**(1), 213-220.

A. Goudarzi, G. M. Aval, R. Sahraei, H. Ahmadpoor(2008), Thin Solid Films **516**, 4953-4957.

A. M. Yildrim, A. Aytunc and A. Aykut, (2009)Physical E. **41**, 1365-1372.

A. U. Ubale and D. K. Kulkarni, (2005) Bul. Mater. Sci., **28**(1), 43-47.

B. Gilbert, B. H. Frazer, H. Zhang, F. Huang, J. F. Banfield, D. Haskel, J. C. Lang, G. Srajer and G. De Stasio, **Phys. Rev**., (2002) **B66**, 245205.

BusarinNoikaew, (2008) PanitaChinvetkitvanich, IntiraSripichai and ChanwitChityuttakan, Journal of Metals, Materials and Minerals, **18**, 2, 49-52.

D. A. Johnston, M. H. Carletto, K. T. R. Reddy, I. Forbes and R. W. Miles(2002), Thin Solid Films **102**, 403-404.

Dong Hyun Hwang, Jung HoonAhn, Kwun Nam Hui, Kwan San Hui and Young Guk Son(2012), Nanoscale Research Letters, **7**(26), 1-7.

F. Lai, M. Li, K. Chen, H. Wang, Y. Song, and Y. Jiang, (2005) Appl. Opt., **44**, 6181-6185.

Huda Abdullah, Norhabibi, Saadah and SahbuddinShaari, (2012) World Applied Sciences Journal **19**(8), 1087-1091.

H. Kashani, (1996) Thin Solid Films **288**, 50.

I. C. Ndukwe, (1996) Solar Energy Materials, **40**, 123-131.

I. O. Oladeji and L. Chow, (1999)Thin Solid Films **339**, 148.

J. Cheng, D. B. Fan, H. Wang, B. W. Liu, Y. C. Zhang and H. Yan, (2003)Semicond. Sci. Technol. **18**, 676.

J. Hasanzadeh, A. Taherkhani and M. Ghorbani, (2013)Chinese Journal of Physics, **51**(3), 540-550.

J. I. Pankove, (1975)"Optical processes in semiconductors", Dover Publications, Inc. New York, pp. 91.

J. M. Dona, J. Herrero, (1994)J. Electrochem. Soc., **141**, 205.

J. Tauc, 1974Amorphous and Liquid Semiconductors New York: plenum press.

J. Vidal, O. Vigil, O. de Melo, N. Lopez and O. Zelaya-Angel, (1999) Mater. Chem. Phys. **61**, 139.

K. L. Chopra, (1969)"Thin Film Phenomena",Mc. Graw Hill BooK Company, USA.

Liang-wen Ji, Yu-Jen Hsiao, I-Tseng Tang, Teen-Hang Meen, Chien-Hung Liu, Jenn-Kai Tsai, Tien-Chuan Wu and Yue-Sian Wu, (2013) Nanoscale Research Letters, **8**(470), 1-6.

L. Lin, F. Lai, Z. Huang, Y. Qu and R. Gai, (2005) 2nd International Symposium on Advanced Optical Manufacturing and Testing Technologies, Proc. Of SPIE, 6149, 614920.

M. Yoneta, M. Ohishi and H. Saito, (1993)J. Cryst. Growth **127**, 314.

M. Y. Nadeem and W. Ahmed, (2000)Turk. J. Phys. **24**:651.

N. KamounAllouche, T. Ben Nasr, N. TurkiKamoun, (2010)G. Guasch, Materials Chemistry and Physics **123**, 620-624.

N. Mehan, V. Gupta, K. Sreenivas and A. Mansingh, (2004)J. Appl. Phys., **96**, 3134-3139.

O. S. Heavens, (1970)"The Film Physics", Methum and Colted.

P. Kathirvel, D. Manoharan, S. M. Mohan and S. Kumar, (2009) J. Optoelectronic and Biomedical Materials **1**, 25-33.

P. K. Nair, M. T. S. Nair, (1992) Semicond. Sci. Technol. **7**, 239.

P. K. Nair, M. T. S. Nair, V. M. Garcia, O. L. Arenas, Y. Pena, A. Castello, I. T. Ayala, O. Gomezdaza, A. Sachez, J. Campos, H. Hu, R. Suarez, M. E. Rincon, (1998) Solar Energy Mater. Solar Cells **52**, 313.

P. O'Brien, D. J. Otway and D. S. Boyle, (2000) Thin Solid Films **17**, 361-362.

P. Roy, J. R. Ota, and S. K. Srivastava, (2006)Thin Solid Films, **515**, 1912-1917.

Q. Liu, M. Guobinh, (2008) A. Jianping, Appl. Surf. Sci., **254**, 5711-5714.

R. F. Louh and W. Wu, (2008) Advanced Materials Research **51**, 125.

R. K. Pandy, S. N. Sahu, S. Chandra, (1996) Hand Book of Semiconductor Electrodeposition, Marcel Dekker, Inc., New York.

R. R. Chamberlin and J. S. Skarman, (1966)J. Electrochem. Soc. **113**, 86.

R. Sahraei, G. MotedayenAval and A. Goudarzi, (2008)J. Alloys Compd. **466**, 488-492.

S. Biswass, P. Pramanik and P. K. Basu, (1986)Mater. Lett. **4**(2), 81.

S. Lindroos, T. Kannianen and M. Leskela, J. Mater. (1996)Chem. **6**(9), 1497.

S. R. Kang, S. W. Shin, D. S. Choi, A. V. Moholkar, J. H. Moon and J. H. Kim, (2010) Current Applied Physics **10**, S437.

S. W. Shin, S. R. Kang, J. H. Yun, A. V. Moholkar, J. H. Moon, J. Y. Lee, J. H. Kim, (2011)Solar Energy Materials and Solar Cells **95**, 856.

S. Yamaga, A. Yoshikawa and H. kasai, (1990) Journal of Crystal Growth, **99**, 432-436.

T. E. Varitimos and R. W. Tustison, (1987)Thin Solid Films, **151**, 27-33.

T. U. Ryu, S. H. Hahn, S. W. Kim and E. J. Kim, (2000) Opt. Eng., **39**, 3207-3213.

Valenzuela AA and Russer P, (1989) Appl. Phys. Lett., **55**, 1029-1031.

Warren BE: (1990)X-ray Diffraction New York: Dover publications.

Xiaochun Wu, (2007) Fachun Lai, Yongzhong Lin, Zhigao Huang and Rong Chen, Proc. Of SPIE, **6722**, 67222L(1-5).

Y. P. V. Subbaiah, P. Prathap, and K. T. R. Reddy, (2006)Appl. Surf. Sci., **253**, 2409-2415.

Z. Porada and E. Schabowska, (1986) Thin Solid Films, **145**, 75.

Z. Q. Li, J. H. Shi, Q. Q. Liu, Z. A. Wang, Z. Sun, S. M. Huang, (2010)Applied Surface Science **257**, 122.

Z. Z. Zhang, D. Z. Shen, J. Y. Zhang, C. X. Shan, Y. M. Lu, Y. C. Liu, B. H. Li, D. X. Zhao, B. Yao, and X. W. Fan, (2006) Thin Solid Films **513**, 114-117.

تأثير المعاملة الحرارية على الخواص التركيبية والضوئية للأغشية الرقيقة لمركب كبريتيد الخارصين ZnS المحضرة بطريقة ترسيب الحمام الكيميائي.

محمـــــد محســـن علي

قسم الفيزياء / كلية العلوم / جامعة البصرة / العراق

حضرت الاغشية الرقيقة لمركب كبريتيد الخارصين ZnS على القواعد الزجاجية باستخدام تقنية ترسيب الحمام الكيميائي (CBD) بدرجة حرارة ترسيب 90^oC للحمام المائي وقد تم معاملة تلك الأغشية الرقيقة حراريا بدرجات حرارية مختلفة (250, 300 and 350^oC) في الهواء وبزمن قدره 30 دقيقة. يحتوي الحمام الكيميائي على محاليل الثيوريا وكبريتات الخارصين والامونيا وهيدرات الهيدرازين. تم التحقق من تأثير درجة حرارة المعاملة الحرارية على خواص التراكيب الدقيقة (المجهرية) والضوئية للأغشية الرقيقة لمركب ZnS . تم تشخيص الخواص التركيبية والضوئية للأغشية الرقيقة لمركب ZnS بواسطة حيود الاشعة السينية ومطياف الأشعة فوق البنفسجية-والمرئية-والقريبة من تحت الحمراء (UV-VIS-NIR) . تشير تحليلات حيود الاشعة السينية الى ان الأغشية الرقيقة لمركب ZnS تمتلك التركيب البلوري المكعب (zinc blende) وبأتجاه نمو مفضل (111) . تم حساب المعاملات التركيبية مثل معامل الشبيكة والحجم البلوري (الحبيبي) والأجهاد الدقيق وكثافة الأنخلاع. نلاحظ تحسن التبلور مع الزيادة بدرجة حرارة المعاملة الحرارية، وقد كان معدل الحجم الحبيبي قبل المعاملة (1.9198 nm) وبعد المعاملة الحرارية اصبح (2.1612 nm) و (4.2821 nm) و (5.7720 nm) على التوالي (وذلك يدل على ان الحجم الحبيبي يزداد بزيادة درجة حرارة التلدين، بينما يقل الاجهاد الدقيق وكثافة الانخلاع مع زيادة درجة حرارة التلدين). كذلك وجدنا تغير سطح الغشاء لمركب ZnS الى ZnO بعد معاملة الأغشية بدرجة حرارة ما بين $300\text{-}350^oC$. تم تسجيل النفاذية والامتصاصية والانعكاسية لأغشية ZnS بمدى الاطوال الموجية 300-1000 nm ، تم حساب فجوة الطاقة للانتقال المباشر وكانت قيمتها 3.85eV ولوحظ نقصان فجوة الطاقة الى 3.42eV مع التلدين. نلاحظ من دراسة النفاذية ان الأغشية الملدنة بدرجة حرارة 350^oC تمتلك أعلى نفاذية بحدود 95.50% . تم حساب معامل الانكسار ومعامل الخمود وكذلك الجزء الحقيقي والجزء الخيالي للثوابت البصرية والتوصيلية الضوئية. أن زيادة درجة حرارة التلدين تعمل على زيادة المسامات في الأغشية، والتي ينتج عنها نقصان في معامل الانكسار وزيادة في معامل الخمود للغشاء.